

# We are IntechOpen, the world's leading publisher of Open Access books Built by scientists, for scientists

4,800

Open access books available

122,000

International authors and editors

135M

Downloads

Our authors are among the

154

Countries delivered to

TOP 1%

most cited scientists

12.2%

Contributors from top 500 universities



WEB OF SCIENCE™

Selection of our books indexed in the Book Citation Index  
in Web of Science™ Core Collection (BKCI)

Interested in publishing with us?  
Contact [book.department@intechopen.com](mailto:book.department@intechopen.com)

Numbers displayed above are based on latest data collected.  
For more information visit [www.intechopen.com](http://www.intechopen.com)



# Time-scaling in the control of mechatronic systems

Bálint Kiss and Emese Szádeczky-Kardoss  
*Budapest University of Technology and Economics*  
Hungary

## 1. Introduction

Time-scaling is not a new concept in the theory of dynamical systems. It has been used to modify the time distribution along the reference paths and also to transform a system by changing the clock with which it evolves. The motivation to introduce time-scaling is often to gain useful properties for the system which evolves according to the modified time. It is shown in (Sampei & Furuta, 1986) that such a property to gain with time-scaling may be feedback linearizability.

The notion of orbital flatness introduced by Fliess et al. (Fliess et al., 1995, 1999) involves also time-scaling to define an equivalence between a class of nonlinear systems and finite chains of integrators. The problem to check the orbital flatness of single input systems is addressed in (Respondek, 1998) and (Guay, 1999) together with the well known example of the kinematic car with constant longitudinal velocity which is shown to be orbitally flat.

The time-scaling introduced by these concepts involves the state variables to express the relation between the different time scales, hence the time-scaling does not involve any new input or variable external to the system.

Another concept for time-scaling is to use the tracking error in closed loop to modify the time-scaling of the reference path (Lévine, 2004). Such methods change the traveling time of the reference path according to the actual tracking error by decelerating if the motion is not accurate enough and by accelerating if the errors are small or vanish.

This chapter presents a new time-scaling scheme which is not driven only by the state variables of the system but also by a new input, referred to as the time-scaling input. In the setup suggested in this chapter, the new input variable, which is not an input of the original physical system, is also used to drive the time-scaling of the reference in closed loop.

The usefulness of our approach is demonstrated for the nonholonomic model of the kinematic car with one input. Notice that solutions to the motion planning and tracking algorithms are reported to the kinematic car with two inputs (Cuesta and Ollero, 2005) exploiting its differentially flatness property or using other methods (Dixon et al., 2001). We show that the kinematic car with one input, such that the longitudinal velocity does not vanish, can track any smooth trajectory with non-vanishing longitudinal velocity such that the tracking error is reduced exponentially along the path. This is achieved using time-scaling and a dynamical feedback similar to the differentially flat case.

The remaining part of the chapter is organized as follows. The next section introduces our new time-scaling concept in details and its application in some general cases. Section 3 addresses the particular problem of the control of a car using its kinematic model such that the only control input is the angle of the steered wheels. Section 4 presents the simulation and real measurement results obtained by the application of the controllers described in Section 3. The conclusion is given in Section 5.

## 2. The time-scaling concept

This section introduces in a general context our novel time-scaling scheme and shows how dynamical systems are transformed by its application. For this reason, consider a finite dimensional and time invariant dynamical system given by its state equation

$$\frac{d\xi}{dt} = \Phi(\xi, u) \quad (1)$$

where  $\xi \in R^n$ ,  $u \in R^m$  are the state vector and the input vector, respectively. This system evolves according to the time  $t$  which we refer to as the real time. Let  $\tau$  denote the scaled time. A time-scaling law is an invertible mapping

$$t \mapsto \tau(t) \quad \tau \mapsto t(\tau). \quad (2)$$

The time-scaling scheme proposed by Sampei and Furuta (Sampei & Furuta, 1986) depends on the state of the system

$$\frac{dt}{d\tau} = s(\xi) \quad \tau(t_0) = \tau_0 \quad (3)$$

and the authors show that the system rewritten according to the time  $\tau$ , namely

$$\frac{d\xi}{d\tau} = \frac{d\xi}{dt} \frac{dt}{d\tau} = s(\xi)\Phi(\xi, u) \quad (4)$$

may exhibit properties which were not satisfied by the system evolving according to the time  $t$ . Such a property studied in the paper is feedback linearizability. Let us point out that the time-scaling defined by (3) does not change the number of inputs of the system. Instead of (3) we introduce a time-scaling concept which increases the number of inputs of the system with a new input referred to as a time-scaling (or simply scaling) input. Hence the time-scaling is driven by

$$\frac{dt}{d\tau} = \sigma(\xi, u_s) \quad \tau(t_0) = \tau_0. \quad (5)$$

This time-scaling results a scaled dynamics

$$\frac{d\xi}{d\tau} = \sigma(\xi, u_s) \Phi(\xi, u) \quad (6)$$

with the inputs  $u$  and  $u_s$ . The same time-scaling can be applied for systems with more specific form of state equation. Considering a driftless system with the state equation

$$\frac{d\xi}{dt} = \sum_{i=1}^m g_i(\xi) u_i \quad (7)$$

the time-scaling (5) results

$$\frac{d\xi}{d\tau} = \sum_{i=1}^m \sigma(\xi, u_s) g_i(\xi) u_i \quad (8)$$

The time-scaling defined by (5) can be generalized by the introduction of a chain of integrators evolving according to the time  $\tau$

$$\frac{dt}{d\tau} = s_1 \quad \frac{ds_1}{d\tau} = s_2 \quad \dots \quad \frac{ds_k}{d\tau} = \sigma(s, \xi, u_s) \quad \tau(t_0) = \tau_0 \quad (9)$$

with  $s = (s_1, s_2, \dots, s_k)$ . Let us now consider the dynamical model of a mechatronic system with  $d$  degrees of freedom such that the  $d$  generalized coordinates are the elements of the vector  $q$ . Such a dynamics reads

$$F_i = \sum_{j=1}^d D_{ij} \ddot{q}_j + \sum_{j=1}^d \sum_{k=1}^d D_{ijk} \dot{q}_j \dot{q}_k + D_i \quad i = 1 \dots d \quad (10)$$

where  $D_{ij}$  are the elements of the inertia tensor,  $D_{ijk}$  are the coefficients of the centripetal and Coriolis effects,  $D_i$  contain the gravitational forces, and  $F_i$  give the generalized

external forces. We use the standard notations  $\dot{q} = \frac{dq}{dt}$ ;  $\ddot{q} = \frac{d^2q}{dt^2}$  and introduce  $q' = \frac{dq}{d\tau}$ ;

$q'' = \frac{d^2q}{d\tau^2}$ . Using simple derivation rules and (9) for  $k=1$ , the relation between the time

derivatives with respect to  $t$  and  $\tau$  read

$$\dot{q} = q' \frac{d\tau}{dt} \quad \ddot{q} = q'' \left( \frac{d\tau}{dt} \right)^2 + q' \frac{d^2\tau}{dt^2} \quad \frac{d^2\tau}{dt^2} = \frac{1}{dt} \frac{1}{s_1} = \frac{d}{d\tau} \left( \frac{1}{s_1} \right) \frac{d\tau}{dt} = - \frac{\sigma(s_1, \xi, u_s)}{s_1^3} \quad (11)$$

which result the following time-scaled system

$$F_i = \sum_{j=1}^d D_{ij} \left( q'' s_1^{-2} - q' \frac{\sigma(s_1, \xi, u_s)}{s_1^3} \right) + \sum_{j=1}^d \sum_{k=1}^d D_{ijk} q'_j q'_k s_1^{-2} + D_i \quad i=1 \dots d \quad (12)$$

subject to (9) and with the state vector  $\xi = (q, \dot{q})$ .

Another possibility for the generalization is to take into account in the model of the dynamical system the effect of some external, but measurable signals. Such signals can be measurable (or estimable) disturbances or one may think of them as input signals which are not generated by the controller but by some other means, e.g. by a human operator. We will denote the vector of these signals by  $w$  which is included in the state equation and can be also incorporated in the time-scaling

$$\frac{d\xi}{dt} = \Phi(\xi, w, u) \quad \frac{dt}{d\tau} = \sigma(\xi, w, u_s) \quad \tau(t_0) = \tau_0 \quad (13)$$

to result a scaled dynamics similar to (6)

$$\frac{d\xi}{d\tau} = \sigma(\xi, w, u_s) \Phi(\xi, w, u) \quad (14)$$

Notice that one reason for the use of the time-scaling can be the elimination of the effect of the external signals in the vector  $w$ .

It is important to note that the time-scaling must not rewind the time, hence (5), (9), and (13) have to be chosen such that the resulting time-scaling law (2) is monotonous.

### 3. Case study: semi-autonomous maneuvering with a passenger car

The time-scaling concept described in the previous section will be applied to the design of a semi-autonomous maneuvering feature for a passenger car. Semi-autonomy means in this case that the controller does not generate all variables that influence the motion of the car, but only a subset of such variables. To be more specific, the driver generates the velocity of the car by the proper actuation of the gas, break, and clutch pedals while the control system determines the angle of the steering wheel. This implies that the geometry of the trajectory can be influenced, but not the traveling time which is needed to complete a given section of the trajectory. Hence the application of the time-scaling introduced in the previous section seems to be natural such that the control objective is to follow a path with the car as the controller can eliminate the geometric error between the desired and the real trajectory.

#### 3.1 Car model

We use the simple kinematic model of the car, also referred to as the one-track or bicycle model in the literature. The model is illustrated in Figure 1 such that the bicycle is fitted on the longitudinal symmetry axis of the car. We suppose that the Ackermann steering

geometry assumption holds true such that all wheels turn around the same point  $P$  which is on the rear axle of the car.

The motion of the car is described by the time functions of its (rear axle midpoint) position  $(x, y)$  and its orientation  $\theta$ . The axle-space of the car is denoted by  $l$ . Two variables influence the motion of the car in the horizontal plane: the longitudinal velocity, denoted by  $v_{car}$ , is generated by the human driver ( $w = v_{car}$ ) and the steering angle  $\varphi$  is the only control input. The kinematic model reads

$$\begin{aligned}\dot{x} &= v_{car} \cos \theta \\ \dot{y} &= v_{car} \sin \theta \\ \dot{\theta} &= \frac{v_{car}}{l} \tan \varphi\end{aligned}\quad (15)$$

It is known from the literature that this model (and its generalized version with trailers) is differentially flat if both  $v_{car}$  and  $\varphi$  are control inputs (Fliess et al., 1995, 1999).

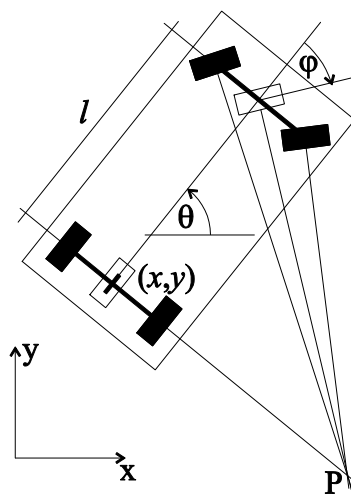


Fig. 1. Bicycle model of a car moving in the horizontal plane

It is also known that for  $v_{car} = 1$  the same model with one input is orbitally flat (Guay, 1999 and Respondek, 1998). Orbital flatness implies the equivalence of the system (15) to a chain of integrators using a transformation which involves dynamic state feedback, coordinate transformation, and time-scaling such that this transformation leaves the number of inputs unchanged.

Using the time-scaling scheme introduced in the previous section we explicitly show how to stabilize a given trajectory for an arbitrary non-vanishing velocity profile  $v_{car}$ .

### 3.2 Model transformation using time-scaling

Since we use a purely kinematic model of the car, the introduction of a time-scaling similar to (13) is sufficient. Moreover, the state variables are not necessary to be included in

the expression which reads in our case (Kiss and Szádezcky-Kardoss, 2007)

$$\frac{dt}{d\tau} = \frac{u_s}{v_{car}} \quad (16)$$

assuming that  $v_{car}$  does not vanish during the trajectory. If  $v_{car}$  and  $u_s$  are both positive (respectively negative) than the resulting time-scaling law does not rewind the time. The dynamics after the application of the time-scaling is given by

$$\begin{aligned} x' &= u_s \cos \theta \\ y' &= u_s \sin \theta \\ \theta' &= \frac{u_s}{l} \tan \varphi \end{aligned} \quad (17)$$

This dynamics, which evolves according to the time  $\tau$ , has two inputs ( $u_s$  and  $\varphi$ ) and it is known to be differentially flat which implies that it is feedback linearizable by dynamic state feedback such that the flat output contains two variables, namely the  $(x, y)$  position of the car.

### 3.3 Asymptotic stabilization of the reference trajectory (according to the time $\tau$ )

Suppose that a reference trajectory  $(x_{ref}, y_{ref})$  is given for the position of the car. A feedback law should be found such that the reference trajectory is asymptotically (or eventually exponentially) tracked. Since the human driver generates the longitudinal velocity of the car, the reference trajectory cannot be designed according to the real time  $t$  but only according to some "virtual" time  $\tau$ .

To understand this fact, consider a reference path with a length of 100 meters and suppose that the time functions  $(x_{ref}(\cdot), y_{ref}(\cdot))$  are determined such that the desired travelling time along the trajectory should be 10 seconds which is a 10 m/s average speed along the path. If the driver generates a constant longitudinal velocity which equals to 20 m/s than the real traveling time (supposing that the tracking is perfect) will be 5 seconds. Similarly, if the driver generates a constant longitudinal velocity which equals to 5 m/s than the real traveling time (supposing again perfect tracking of the geometry of the path) will be 20 seconds. Moreover, the velocity profile for a given maneuver is not know in advance so the time-scaling must use the current velocity value generated by the driver and eventually its time derivatives.

It follows that one cannot design a controller which ensures a desired travelling time, according to the real time  $t$ , but it is possible with respect to the "virtual" time  $\tau$ . So we will suppose that the reference  $(x_{ref}(\tau), y_{ref}(\tau))$  is given according to  $\tau$  and the designed controller is able to ensure the asymptotic stabilization according to the same virtual time  $\tau$ . The reference is given by the mapping

$$\begin{aligned}\tau &\mapsto \{x_{ref}, x'_{ref}, x''_{ref}, x'''_{ref}\} \\ \tau &\mapsto \{y_{ref}, y'_{ref}, y''_{ref}, y'''_{ref}\}\end{aligned}\quad (18)$$

for  $\tau \in [0, T]$  where  $T$  is the desired traveling time along the trajectory according to the time  $\tau$ . The control loop is depicted in Figure 2.

Let us define the tracking error as  $e_x = x - x_{ref}$  and  $e_y = y - y_{ref}$ . The closed loop system must guaranty the exponential decay of the tracking errors according to the time  $\tau$  so the following equations

$$\begin{aligned}k_{x,0}e_x + k_{x,1}e'_x + k_{x,2}e''_x + e'''_x &= 0 \\ k_{y,0}e_y + k_{y,1}e'_y + k_{y,2}e''_y + e'''_y &= 0\end{aligned}\quad (19)$$

must be satisfied such that the coefficients  $k_{a,i}$  ( $a \in \{x, y\}, i = 0, 1, 2$ ) are design parameters and have to be chosen such that the characteristic polynomials of (19) are Hurwitz.

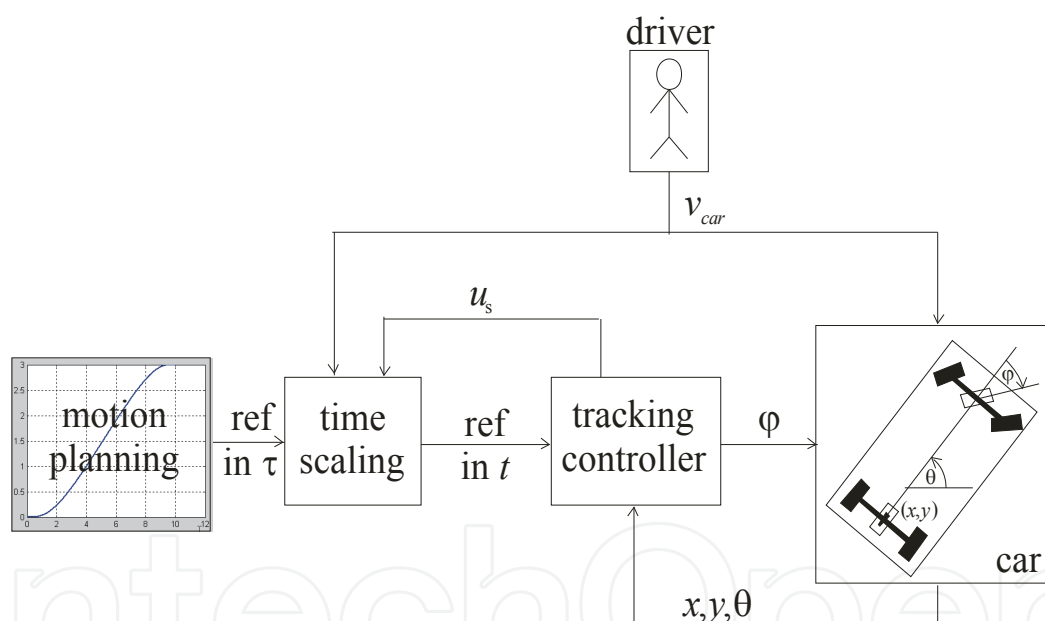


Fig. 2. Scheme of the control loop including the tracking controller and the time-scaling

The following calculations are based on the differential flatness property of (17) which implies that the model can be linearized by a dynamic state feedback.

In order to satisfy (19) we first add some integrators in front of both inputs of (17). These integrators are realized in the controller and the new inputs of the integrator chains are  $v_1$  and  $v_2$ .

$$\begin{aligned}\zeta'_1 &= \zeta_2 = u'_s & \zeta'_3 &= v_2 \\ \zeta'_2 &= v_1 = u''_s & \varphi &= \zeta_3 \\ u_s &= \zeta_1\end{aligned}\quad (20)$$



Note that one could add more integrators and the minimal number of integrators such that the calculations that follow can be carried out is one preceding the  $u_s$  input. The chains of integrators are illustrated in Figure 3.

Using the states of (17) and the states of the dynamic extension (20), the derivatives  $x'$ ,  $x''$ ,  $x'''$ ,  $y'$ ,  $y''$ ,  $y'''$  can be determined.

$$x' = \zeta_1 \cos \theta \quad (21)$$

$$x'' = \zeta_2 \cos \theta - \frac{\zeta_1^2 \sin \theta \tan \zeta_3}{l} \quad (22)$$

$$x''' = v_1 \cos \theta - \frac{3\zeta_1\zeta_2 \sin \theta \sin \zeta_3}{l \cos \zeta_3} - \frac{\zeta_1^3 \cos \theta}{l^2 (\cos \zeta_3)^2} + \frac{\zeta_1^3 \cos \theta}{l^2} - \frac{v_2 \zeta_1^2 \sin \theta}{l (\cos \zeta_3)^2} \quad (23)$$

$$y' = \zeta_1 \sin \theta \quad (24)$$

$$y'' = \zeta_2 \sin \theta + \frac{\zeta_1^2 \cos \theta \tan \zeta_3}{l} \quad (25)$$

$$y''' = v_1 \sin \theta + \frac{3\zeta_1\zeta_2 \cos \theta \sin \zeta_3}{l \cos \zeta_3} - \frac{\zeta_1^3 \sin \theta}{l^2 (\cos \zeta_3)^2} + \frac{\zeta_1^3 \sin \theta}{l^2} + \frac{v_2 \zeta_1^2 \cos \theta}{l (\cos \zeta_3)^2} \quad (26)$$

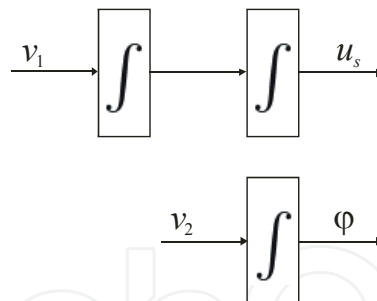


Fig. 3. Integrators (dynamic extension) in the controller

The inputs of the integrator chains of Figure 3 ( $v_1$  and  $v_2$ ) appear in the expressions of  $x'''$  (23) and  $y'''$  (26). This implies that one can calculate them such that the linear differential equations for the tracking errors (19) are satisfied. To achieve this, isolate first  $x'''$  and  $y'''$  from (19) to obtain

$$\begin{aligned} x''' &= x'''_{ref} - k_{x,0}e_x - k_{x,1}e'_x - k_{x,2}e''_x = \omega_x \\ y''' &= y'''_{ref} - k_{y,0}e_y - k_{y,1}e'_y - k_{y,2}e''_y = \omega_y \end{aligned} \quad (27)$$

Combining (23) and (26) with (27) one gets

$$\begin{bmatrix} \cos \theta & -\frac{\zeta_1^2 \sin \theta}{l(\cos \zeta_3)^2} \\ \sin \theta & \frac{\zeta_1^2 \cos \theta}{l(\cos \zeta_3)^2} \end{bmatrix} \begin{bmatrix} v_1 \\ v_2 \end{bmatrix} = \begin{bmatrix} \omega_x - A \\ \omega_y - B \end{bmatrix} \quad (28)$$

with

$$\begin{bmatrix} A \\ B \end{bmatrix} = \begin{bmatrix} -\frac{3\zeta_1\zeta_2 \sin \theta \sin \zeta_3}{l \cos \zeta_3} - \frac{\zeta_1^3 \cos \theta}{l^2(\cos \zeta_3)^2} + \frac{\zeta_1^3 \cos \theta}{l^2} \\ \frac{3\zeta_1\zeta_2 \cos \theta \sin \zeta_3}{l \cos \zeta_3} - \frac{\zeta_1^3 \sin \theta}{l^2(\cos \zeta_3)^2} + \frac{\zeta_1^3 \sin \theta}{l^2} \end{bmatrix} \quad (29)$$

Finally, the inputs  $v_1$  and  $v_2$  are obtained by the inversion of the coefficient matrix in (28)

$$\begin{bmatrix} v_1 \\ v_2 \end{bmatrix} = \begin{bmatrix} \cos \theta & \sin \theta \\ -\frac{l \sin \theta (\cos \zeta_3)^2}{\zeta_1^2} & \frac{l \cos \theta (\cos \zeta_3)^2}{\zeta_1^2} \end{bmatrix} \begin{bmatrix} \omega_x - A \\ \omega_y - B \end{bmatrix} \quad (30)$$

The coefficient matrix is singular if  $\zeta_1 = u_s = 0$  which occurs at zero longitudinal velocity. Another singularity occurs if  $\zeta_3 = \varphi = \pm 90^\circ$ . Singularities coincide with the loss of controllability of the model.

Based on the previous calculations, the reference trajectory (18), the states of the kinematic car (17) and the states of the dynamic extension (20) allow determining the inputs  $v_1$  and  $v_2$  of the system extended by the integrators and thus to obtain the time-scaling input  $u_s$  and the steering angle  $\varphi$  which results the exponential stabilization of the reference trajectory.

### 3.4 Time-scaling of time functions

Expressions (21)-(26) hold true if the variables on the left hand sides are functions of  $\tau$ . Notice however that the measured states of the car evolve with the real time  $t$  so the time derivatives with respect to  $\tau$  cannot be directly determined. Therefore one needs the transformation which allows mapping a time function of  $t$  and its derivatives to a time function of  $\tau$  and to its derivatives using the time-scaling law specified by (16). Consider a variable  $\alpha$ . We wish to obtain the mapping

$$\{\alpha(t), \dot{\alpha}, \ddot{\alpha}, \dots\} \leftrightarrow \{\alpha(\tau), \alpha', \alpha'', \dots\} \quad (31)$$

The time-scaling law (2) can be obtained by the integration of (16) and reads in our case

$$\tau(t) = \int_0^t \frac{v_{car}}{u_s} d\mathcal{G} \quad \tau(0) = t(0) = 0 \quad (32)$$

which allows expressing the transformation (31) as

$$\alpha(t) = \alpha(\tau(t)) \quad (33)$$

$$\dot{\alpha}(t) = \alpha'(\tau(t))\dot{\tau} \quad (34)$$

$$\ddot{\alpha}(t) = \alpha''(\tau(t))\dot{\tau}^2 + \alpha'(\tau(t))\ddot{\tau} \quad (35)$$

$$\dddot{\alpha}(t) = \alpha'''(\tau(t))\dot{\tau}^3 + 3\alpha''(\tau(t))\dot{\tau}\ddot{\tau} + \alpha'(\tau(t))\dddot{\tau} \quad (36)$$

The successive time derivatives ( $\dot{\tau}, \ddot{\tau}, \dddot{\tau}$ ) of the time-scaling law (32) can be also obtained using the time derivatives of  $v_{car}$  and the time derivatives of  $u_s$ .

$$v_{car} = \dot{u}_s \quad (37)$$

$$\dot{v}_{car} = \ddot{u}_s + \dot{\tau}^2 u'_s \quad (38)$$

$$\ddot{v}_{car} = \dddot{u}_s + 3\dot{\tau}\ddot{u}'_s + \dot{\tau}^3 u''_s \quad (39)$$

We suppose that the time derivatives of  $v_{car}$  can be measured or estimated. The time derivatives of  $u_s$  are the states of the dynamic extension (20).

### 3.5 Stabilization using linearized error dynamics

The method presented in the previous subsection required the time derivatives of  $v_{car}$  but their measurement or estimation may present difficulties. We propose therefore an alternative stabilization technique which overcomes this difficulty. The price to pay is that the stability will be only locally achieved since the feedback is based on the linearized error dynamics. The method is derived from the results presented in (Dixon et al., 2001).

We suppose that the reference time functions of all variables ( $x_{ref}, y_{ref}, \theta_{ref}, u_{s,ref}, \varphi_{ref}$ ) are given such that they satisfy the model (17).

Let us define the error variables  $e_x = x - x_{ref}$ ,  $e_y = y - y_{ref}$ ,  $e_\theta = \theta - \theta_{ref}$  and the error transformation

$$\begin{bmatrix} e_1 \\ e_2 \\ e_3 \end{bmatrix} = \begin{bmatrix} \cos \theta & \sin \theta & 0 \\ -\sin \theta & \cos \theta & 0 \\ 0 & 0 & 1 \end{bmatrix} \begin{bmatrix} e_x \\ e_y \\ e_\theta \end{bmatrix} \quad (40)$$

which can be used to express the error dynamics as

$$\begin{bmatrix} \dot{e}_1 \\ \dot{e}_2 \\ \dot{e}_3 \end{bmatrix} = \begin{bmatrix} 0 & \dot{\theta} & 0 \\ -\dot{\theta} & 0 & 0 \\ 0 & 0 & 0 \end{bmatrix} \begin{bmatrix} e_1 \\ e_2 \\ e_3 \end{bmatrix} + \begin{bmatrix} 0 \\ \sin e_3 \\ 0 \end{bmatrix} u_{s,ref} \frac{v_{car}}{u_s} + \begin{bmatrix} 1 & 0 \\ 0 & 0 \\ 0 & 1 \end{bmatrix} \begin{bmatrix} w_1 \\ w_2 \end{bmatrix} \quad (41)$$

with the inputs  $w_1$  and  $w_2$  obtained as

$$w_1 = v_{car} - \frac{v_{car}}{u_s} u_{s,ref} \cos e_3 \quad (42)$$

$$w_2 = \frac{1}{l} \left( v_{car} \tan \varphi - \frac{v_{car}}{u_s} u_{s,ref} \tan \varphi_{ref} \right) \quad (43)$$

The expressions (42)-(43) also show how to calculate  $u_s$ ,  $\dot{\theta}$ , and  $\varphi$  from  $w_1$  and  $w_2$ . The error dynamics (41) can be linearized around zero error and zero inputs (which implies that  $\dot{\theta} = 0$  in (41)) and a state-feedback (pole-placement)

$$\begin{bmatrix} w_1 \\ w_2 \end{bmatrix} = -K \begin{bmatrix} e_1 \\ e_2 \\ e_3 \end{bmatrix} \quad (44)$$

can be used to stabilize the system around the reference trajectory.

## 4. Simulation and measurement results

Both stabilizing feedback laws presented in Section 3 are implemented in Matlab-Simulink<sup>1</sup> environment. The controller described in Subsection 3.3 is also implemented in a Ford Focus type passenger car using the rapid control prototyping environment comprising Matlab-Simulink, the Real-Time Workshop together with DSpace<sup>2</sup> Autobox hardware connected to the CAN bus of the car. The vehicle is equipped with a special prototype of an Electronic Power Assist Steering (EPAS) System developed by our industrial partner. This EPAS can receive and precisely track a reference for the steering angle (denoted by  $\varphi$  in our model) sent via the CAN bus of the vehicle.

### 4.1 Simulation results

For the simulation we use the simple kinematic model of the car as given by Equation (15) with  $l=1$  m. A lane-changing-like maneuver is the reference such that the lane-change

<sup>1</sup> <http://www.mathworks.com>

<sup>2</sup> <http://www.dspace.de>

represents a 3.5 meters shift to the lateral direction while advancing 10 meters. The motion planning was carried out with a default velocity profile which is referred to as the reference driver with a travelling time of 9 seconds. To demonstrate the time-scaling in simulation, we generated two additional velocity profiles such that the first is quicker and the second is slower than the reference driver. These three velocity profiles are depicted in Figure 4-a. The figure also shows the different traveling times necessary to complete the lane-changing maneuver for each velocity profile.

To check the asymptotic tracking property of the controller presented in Subsection 3.3 we set an initial position and orientation which is different from the ones used for motion planning such that the initial tracking errors are  $e_x = -1.5$  m,  $e_y = 2$  m, and  $e_\theta = \pi/4$  rad. Due to time-scaling, the geometries of the trajectories in both cases (quick and slow drivers) are the same in the horizontal plane as shown in Figure 4-b. All trajectories converge to the reference despite the relatively large initial errors.

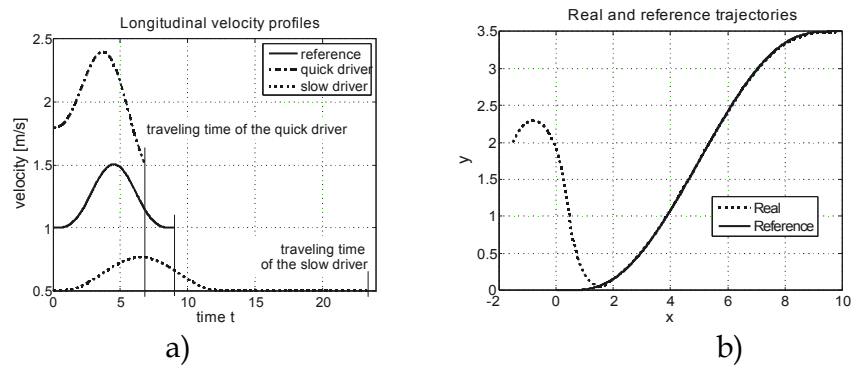


Fig. 4. a) Velocity profiles; b) Reference and real trajectories (same for all velocity profiles)

The time-scaling is shown in Figure 5. It can be seen that the same amount of “virtual” time  $\tau$  (9 seconds) is needed to complete the maneuver but in terms of real time, the driver with quick velocity profile required around 7 seconds and the driver with slow velocity profile required more than 20 seconds completing the same trajectory.

Figure 5-b shows when the reference in  $\tau$  was decelerated or accelerated with respect to the real time  $t$ . It is interesting to see that the reference was decelerated even for the quick driver while the tracking error was large enough.

The steering angles produced by the controller are shown in Figure 6.

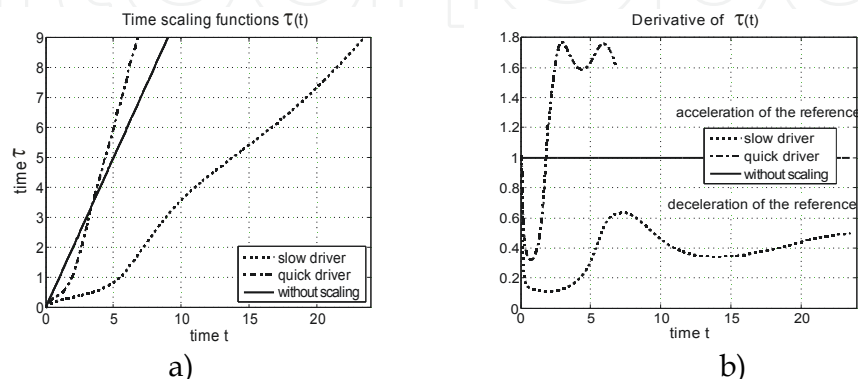


Fig. 5. Time-scaling for the different velocity profiles; a) function  $\tau(t)$ ; b) function  $\dot{\tau}(t)$

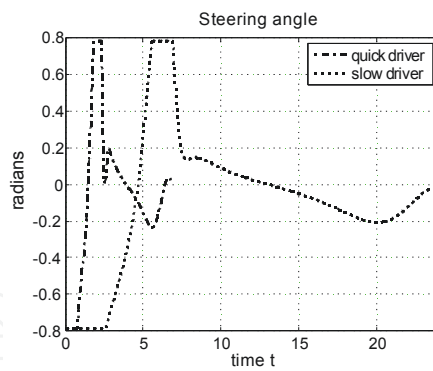


Fig 6. Steering angles during the maneuvers

We carried out similar simulation studies for the controller based on the linearized error dynamics described in Subsection 3.5. The controller locally stabilizes the reference trajectory so the initial errors were chosen to be smaller as in the previous case:  $e_x = -0.5$  m,  $e_y = 0.75$  m, and  $e_\theta = \pi/4$  rad.

The velocity profiles and the geometry of the path are depicted in Figure 7. The time-scaling function  $\tau(t)$  and its derivative are shown in Figure 8. Notice again that the time is decelerated first due to the relatively large tracking error.

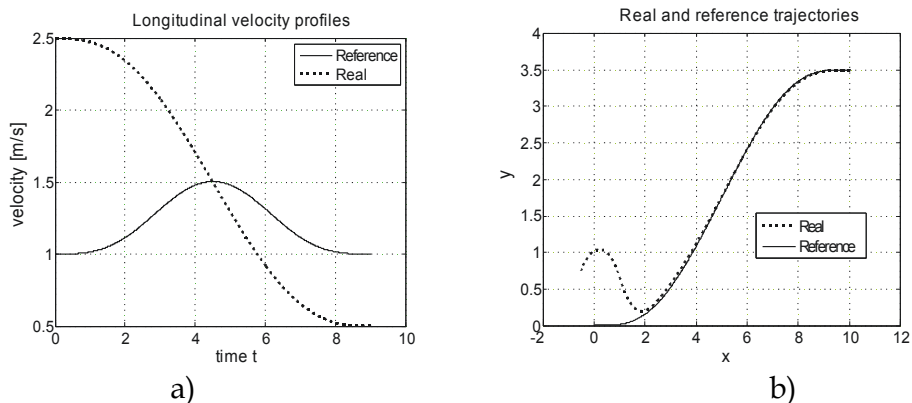


Fig. 7. Performance of the controller designed for the linearized error dynamics; a) velocity profiles; b) Real and reference trajectories in the horizontal plane

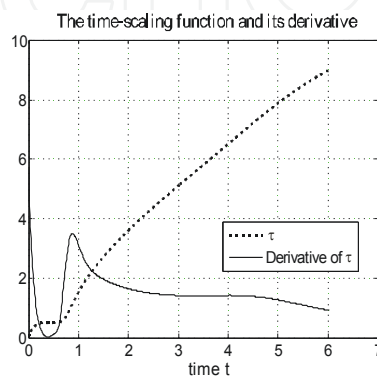


Fig. 8. Time-scaling function and its derivative.

#### 4.2 Measurement results

The controller is implemented in a real passenger car with 10ms sampling time. Figure 9 shows the Ford Focus type test vehicle with the Autobox. The position and orientation of the car is estimated using the ABS wheel sensors the signals of which are available on the CAN bus of the vehicle. The description of the estimation algorithm is beyond the scope of this chapter, for similar algorithms the reader may refer to (Kochen et al., 2002).

The controller is applied here to track trajectories in parking scenarios. Two examples are studied. The first is the case of a parallel parking maneuver in backward direction where an initial position error was introduced as shown in Figure 10-a. The velocity profile generated by the driver (as measured on the CAN bus of the vehicle) and the steering wheel angle generated by the controller (in degrees) are depicted in Figure 10-b. Notice that the special EPAS which is built in the vehicle receives the steering wheel angle and not directly the angle denoted by  $\varphi$ .

The second example is a backward direction perpendicular parking maneuver (see Figure 11-a) with an initial error in position and orientation which is so large that the steering input is saturated during the motion as shown in Figure 11-b. Despite the saturation of the input, the reference trajectory is joined by the vehicle and the initial error is eliminated.



Fig. 9. The Ford Focus test vehicle; a) the DSpace Autobox in the carrier, connected to the CAN bus; b) a possible reference trajectory for a parking maneuver

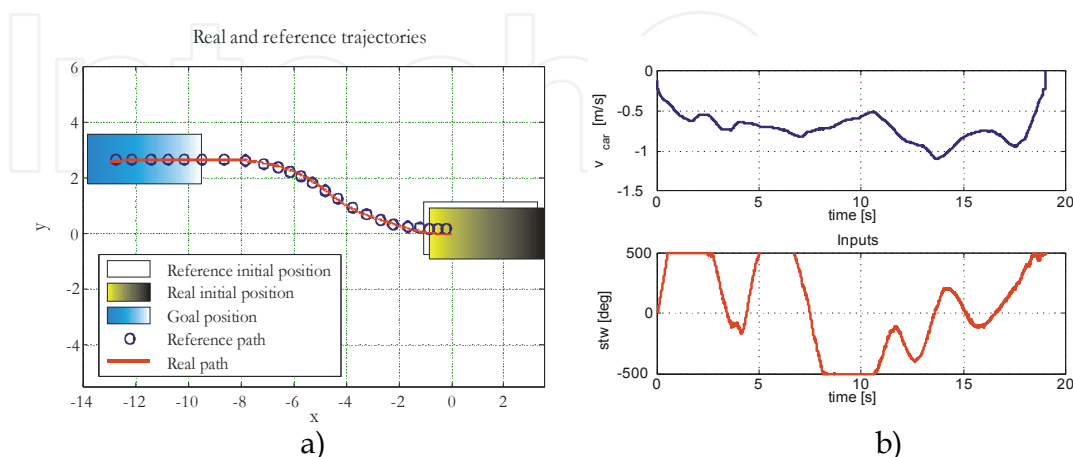


Fig. 10. Backward direction parallel parking maneuver with the Ford Focus; a) Trajectory in the horizontal plane; b) Driver's velocity profile and the steering wheel angle generated by the controller

## 5. Conclusion

This chapter presented a new time-scaling scheme applicable to the control of dynamical systems. The novelty resides in the fact that, in addition to the state variables, the time-scaling is influenced by a new variable which becomes an additional input of the time-scaled system. No general result is formulated at the time being concerning the properties of this time-scaling scheme but it turns out to be useful for a particular application, namely in the semi-autonomous control of a passenger car such that the velocity is generated by the driver but the steering action is determined by the controller.

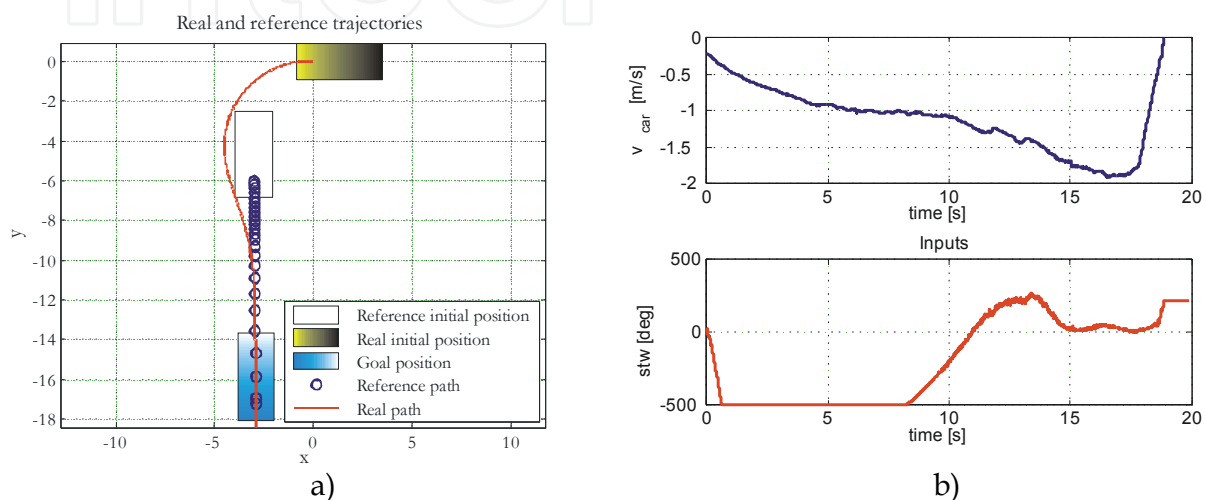


Fig. 11. Backward direction perpendicular parking maneuver with the Ford Focus; a) Trajectory in the horizontal plane; b) Driver's velocity profile and the steering wheel angle generated by the controller

## 6. Acknowledgements

The research was partially funded by the Hungarian Science Research Fund under Grant OTKA K71762 and by the Advanced Vehicles and Vehicle Control Knowledge Center under grant RET 04/2004.

## 7. References

- Cuesta, F. & Ollero., A. (2005). Intelligent Mobile Robot Navigation, *ser. Springer Tracts in Advanced Robotics*. Vol. 16, ISBN 3540239561, Springer, 2005.
- Dixon, W.E.; Dawson, D.M.; Zergeroglu, E. & Behal, A. (2001). Nonlinear control of wheeled mobile robots, *Lecture Notes in Control and Information Sciences*. Vol. 262, ISBN: 978-1-85233-414-7, Springer, 2001.
- Fliess, M.; Lévine, J. ; Martin, Ph. & Rouchon, P. (1995). Flatness and Defect of Nonlinear Systems: Introductory Theory and Examples. *International Journal of Control*, Vol. 61, No. 6, June, 1995, pp. 1327-1361, ISSN: 0020-7179



- Fliess, M.; Lévine, J.; Martin, Ph. & Rouchon, P. (1999). A Lie-Bäcklund Approach to Equivalence and Flatness of Nonlinear Systems. *IEEE Transactions on Automatic Control*, Vol. 44, No. 5, May, 1999, pp. 922-937, ISSN 0018-9286
- Guay, M. (1999). An algorithm for orbital feedback linearization of single-input control affine systems. *Systems & Control Letters*, Vol. 38, No. 4, December, 1999, pp. 271-281, ISSN 0167-6911
- Kiss, B. & Szádeczky-Kardoss, E. (2007). Tracking control of the orbitally flat kinematic car with a new time-scaling input. *Proceedings of the 46th Conference on Decision and Control*, pp. 1969-1974, ISBN 1-4244-1498-9, New Orleans LA, December 2008, IEEE
- Kochen, M.; Neddenriep, R.; Isermann, R.; Wagner, N. & Hamann C-D. (2002). Accurate local vehicle dead-reckoning for a parking assistance system. *Proceedings of the American Control Conference*, pp. 4297-4302, ISBN 0-7803-7298-0, Anchorage AK, May 2002, IEEE
- Lévine, J. (2004). On the Synchronization of a Pair of Independent Windshield Wipers. *IEEE Transactions on Control Systems Technology*, Vol. 12, No. 5, 2004, pp. 787-795, ISSN 1558-0865
- Respondek, W. (1998). Orbital feedback linearization of single-input nonlinear control systems, *Proceedings of the 4th IFAC Nonlinear Control Systems Design Symposium*, pp. 499-504, ISBN: 0-08-043049-X, Enschede, The Netherlands, July 1998, IFAC
- Sampei, M. & Furuta, K. (1986). On Time Scaling for Nonlinear Systems: Application to Linearization. *IEEE Transactions on Automatic Control*, Vol. AC-31, No. 5, May, 1986, pp. 459-462, ISSN 0018-9286

IntechOpen



## **New Developments in Robotics Automation and Control**

Edited by Aleksandar Lazinica

ISBN 978-953-7619-20-6

Hard cover, 450 pages

**Publisher** InTech

**Published online** 01, October, 2008

**Published in print edition** October, 2008

This book represents the contributions of the top researchers in the field of robotics, automation and control and will serve as a valuable tool for professionals in these interdisciplinary fields. It consists of 25 chapters that introduce both basic research and advanced developments covering the topics such as kinematics, dynamic analysis, accuracy, optimization design, modelling, simulation and control. Without a doubt, the book covers a great deal of recent research, and as such it works as a valuable source for researchers interested in the involved subjects.

### **How to reference**

In order to correctly reference this scholarly work, feel free to copy and paste the following:

Balint Kiss and Emese Szadeczky-Kardoss (2008). Time-scaling in the Control of Mechatronic Systems, *New Developments in Robotics Automation and Control*, Aleksandar Lazinica (Ed.), ISBN: 978-953-7619-20-6, InTech, Available from:

[http://www.intechopen.com/books/new\\_developments\\_in\\_robotics\\_automation\\_and\\_control/time-scaling\\_in\\_the\\_control\\_of\\_mechatronic\\_systems](http://www.intechopen.com/books/new_developments_in_robotics_automation_and_control/time-scaling_in_the_control_of_mechatronic_systems)

# **INTECH**

open science | open minds

### **InTech Europe**

University Campus STeP Ri  
Slavka Krautzeka 83/A  
51000 Rijeka, Croatia  
Phone: +385 (51) 770 447  
Fax: +385 (51) 686 166  
[www.intechopen.com](http://www.intechopen.com)

### **InTech China**

Unit 405, Office Block, Hotel Equatorial Shanghai  
No.65, Yan An Road (West), Shanghai, 200040, China  
中国上海市延安西路65号上海国际贵都大饭店办公楼405单元  
Phone: +86-21-62489820  
Fax: +86-21-62489821

© 2008 The Author(s). Licensee IntechOpen. This chapter is distributed under the terms of the [Creative Commons Attribution-NonCommercial-ShareAlike-3.0 License](#), which permits use, distribution and reproduction for non-commercial purposes, provided the original is properly cited and derivative works building on this content are distributed under the same license.

IntechOpen

IntechOpen